THE PbS-Si HETEROJUNCTION: A NEW APPROACH TO INFRARED FOCAL PLANE ARRAY INTEGRATION

A.J. Steckl, M.E. Motamedi, S.P. Sheu, H. Elabd, and K.Y. Tam

Rensselaer Polytechnic Institute - Troy, N. Y. 12181

Abstract

A novel approach to IR focal plane array integration, the PbS-Si Heterojunction, is presented. The PbS-Si HJ structure and basic electrical properties are discussed. The IR detection properties of isotype and anisotype HJ's are covered mainly in the current mode operation. Detectivity levels higher than 10^{11} cm $\sqrt{Hz}/W$ are reported at 85°K and 2 Hz. The integration of the HJ with either a CCD or MOS switch array is discussed. An experimental CMOS chip designed to evaluate the PbS-Si HJ focal plane array is presented.

I. Introduction

The current work in the area of the monolithic integration of large scale infrared focal plane arrays with a solid state self-scanned read-out mechanism is centered on the use of charge coupled devices [1]. The two basic approaches receiving most attention are direct extensions of the original charge transfer concept: a) the use of an MOS structure built around a narrow bandgap semiconductor substrate; b) the use of an MOS structure built around a Si substrate doped with shallow, IR-sensitive impurities.

In this paper, we discuss a novel approach: the thin film narrow gap semiconductor - Si heterojunction. In the heterojunction approach, IR photons are absorbed in the narrow gap thin film. The resulting photocarriers are injected into the Si substrate where they are first accumulated at individual storage sites and then transferred out by a CCD shift register. Alternatively, the read-out can be performed by an array of MOS switches in which case random as well as serial read-out can be achieved. The principal advantages to be derived from this approach are due to the fact that in the heterostructure the photogeneration and read-out processes are separated and performed in materials appropriate for each function. First, the detection takes place in the narrow bandgap semiconductor requiring only a thin film of no more than a few microns. Second, the charge transfer process takes place in a CCD structure fabricated on standard Si material, thus fully utilizing the advantages of IC technology.

The advantages of the heterojunction approach can be realized, however, only if the detection properties of the basic heterojunction are competitive with state-of-art IR detectors. In this paper we will discuss the operation and characteristics of the PbS-Si heterojunction (HJ) detector and its application to focal plane integration.

II. PbS-Si HJ: Structure and Basic Properties

The PbS-Si HJ is formed by growing, at room temperature, a PbS film from chemical solution onto a silicon substrate. Constituents of the chemical solution growth technique [2], [3], [4]are the following: Lead Nitrate($Pb(NO_3)_2$), Sodium Hydroxide (NaOH), Thiourea ($(NH_2)_2$ CS) and Deionized Water. The growth reaction results in a PbS film in intimate and continuous contact with the silicon substrate, as can be seen in the SEM photograph of Fig. 1. The

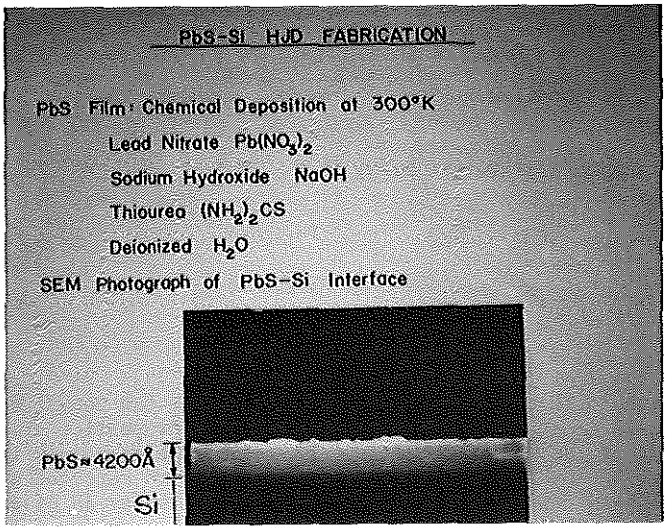

Fig. 1 PbS-Si HJ Fabrication

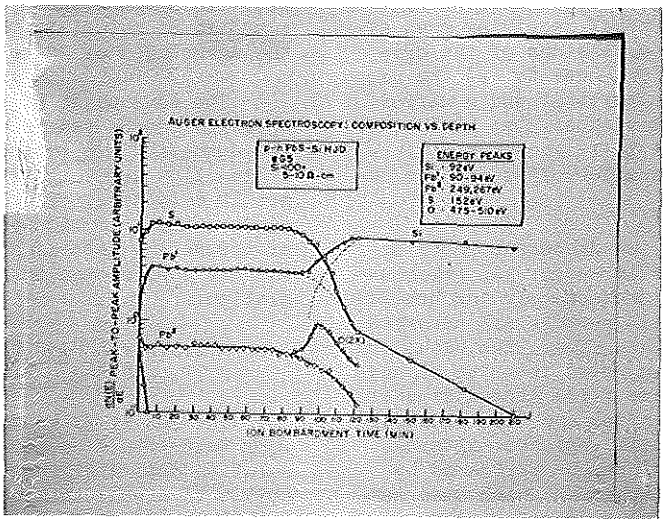

Fig. 2 Auger Electron Spectroscopy

PbS films grown by this method have been shown by X-ray diffraction to be polycrystalline. We have successfully delineated the PbS crystallite pattern using a heat treatment technique [5]. The average grain size in the plane of the substrate has been determined to be around 2500Å. The basic chemical composition and uniformity of the PbS film was investigated by Auger Electron Spectroscopy. An example is shown in Fig. 2 for a PbS film grown on (100) Si. A uniform film composition and a fairly abrupt junction are observed. The O_2 peak of the interface can be attributed to either traces of SiO_2, PbO or surface absorbed oxygen.

The PbS films grown by chemical solution growth have been found to be p-type. Therefore, either isotype [6] (p-p) HJ's or anisotype [7] (p-n) HJ's can be obtained by choosing either p or n-type Si as a substrate. The basic electrical properties of the PbS-Si HJ can be studied from the current voltage (I-V) and capacitance-voltage (C-V) characteristics. In Fig. 3 is shown a typical I-V characteristic of a p-p PbS-Si HJ at 77°K. This device has an area of $6 \times 10^{-4} cm^2$. The extremely small leakage current and sharp turn-on characteristics are indicative of the high quality of our devices. In Fig. 4 is shown the C-V characteristic of a PbS-Si HJD at both 77°K and 300°K. The data is plotted in the usual $1/C^2$ vs. V format. The linear relationship under reverse bias follows the theoretical characteristic and is therefore also indicative of the quality of the HJD.

III. IR Detector Characteristics

We have found that the PbS-Si HJ exhibits substantial IR sensitivity in both isotype [6] and anisotype [7] form when operated in either the voltage (open circuit) mode or the current mode [8]. In this paper, we will highlight the properties of the p-n PbS-Si HJ operated in the current mode at a temperature of 80 to 85°K. It is worthwhile to note that we have achieved a detectivity of over $10^{11} cm\sqrt{Hz}/W$ in the 2.5-3.0μm region.

The photocurrent signal measurements were performed on the blackbody test station illustrated in Fig. 5. In Fig. 6, the photocurrent is plotted versus power density for different values of bias at a signal frequency of 10 Hz. The photocurrent is seen to increase a factor of 3-5 when the bias is raised from zero volts to -50 mV. To obtain the same factor of signal improvement again one has to increase the bias to between -1 V to -2 V. It is important to note that the linear region of the photocurrent vs. power curve is extended as one increases the bias. The frequency response of the photocurrent as a function of bias level is shown in Fig. 7.

Current noise measurements have been performed as a function of frequency and bias. These measurements require considerable care due to the very low level of noise generated by the HJD. In Fig. 8, the current noise at zero bias and at -50 mV bias is shown as a function of frequency. It is important to note that the noise for both bias levels is essentially the same over the entire range measured, 2 Hz to 1 kHz. As shown above, the signal at -50 mV is between three to five times higher than at zero bias. It can also be seen from the data that no 1/f noise component was observed in either case down to a frequency of 2 Hz. The preamp current noise is also plotted separately in Fig. 8. Due to the very low noise of the HJD, the total noise measured in the 2-10 Hz range is very close to being preamp noise limited. For example, at 2 Hz and -50 mV the total current noise measured is 5 fA Hz. The preamp noise was measured to be $3.5\ fA/\sqrt{Hz}$ resulting in a calculated detector-only current noise of also $3.5\ fA/\sqrt{Hz}$.

The blackbody detectivity has been calculated from the signal and noise data presented above. In Fig. 9, the blackbody detectivity is plotted versus frequency at zero bias and -50 mV. At a frequency of 2 Hz and -50 mV bias we obtain a detectivity of $1.8 \times 10^{11} cm\sqrt{Hz}/W$ while for zero bias and 2 Hz a $D^*_{BB} = 6 \times 10^{10} cm\sqrt{Hz}/W$ is obtained. The relatively high reproducibility of the PbS-Si HJ detectivity is exemplified in Fig. 10, where D^*_{BB} is plotted versus frequency for two detectors held at the same bias level of -50 mV. The spectral response of the HJD was measured on the test station illustrated in Fig. 11. The spectral response of the p-n PbS-Si HJD operated in the current mode and with zero bias is shown in Fig. 12. In Fig. 13, the spectral detectivity is plotted at a frequency of 2 Hz and a reverse bias of 50 mV. In the spectral region of interest, 2.5-3.0 μm, D^*_λ is around $10^{11} cm\sqrt{Hz}/W$. At λ = 2.75μm the conversion factor from blackbody to spectral detectivity is approximate-

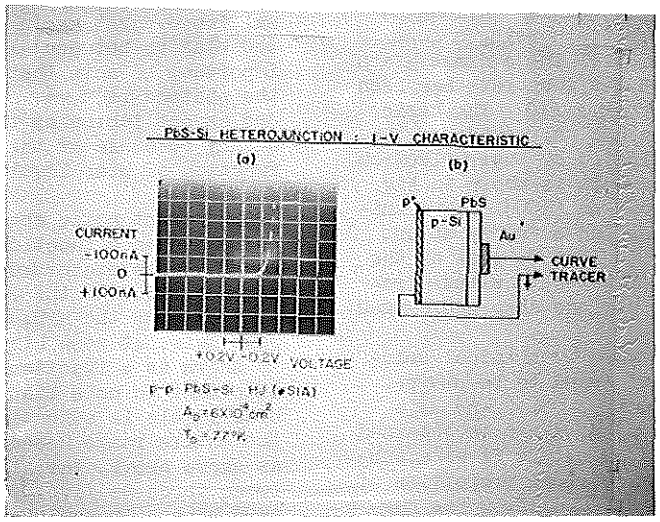

Fig. 3. p-p PbS-Si HJ: I-V Characteristic

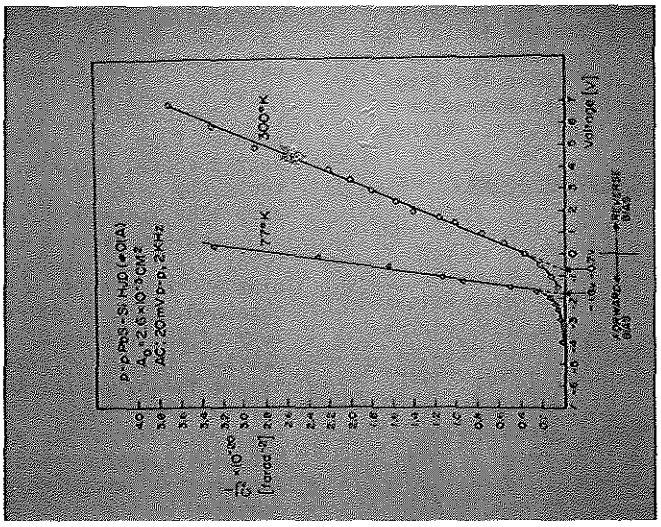

Fig. 4 p-p PbS-Si HJ: C-V Characteristic

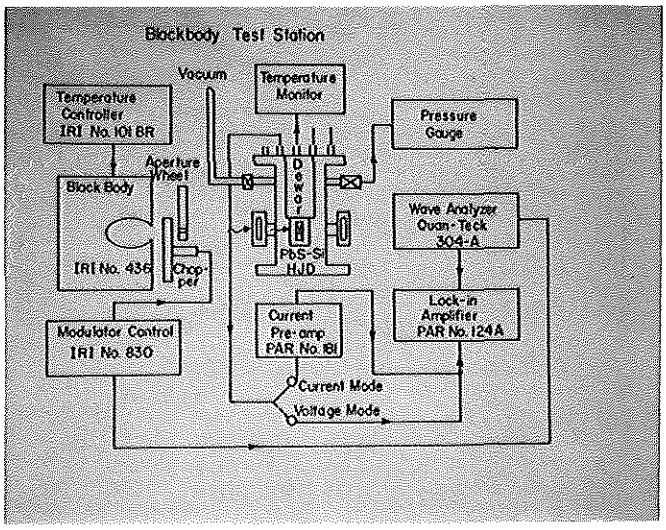

Fig. 5 Blackbody Test Station

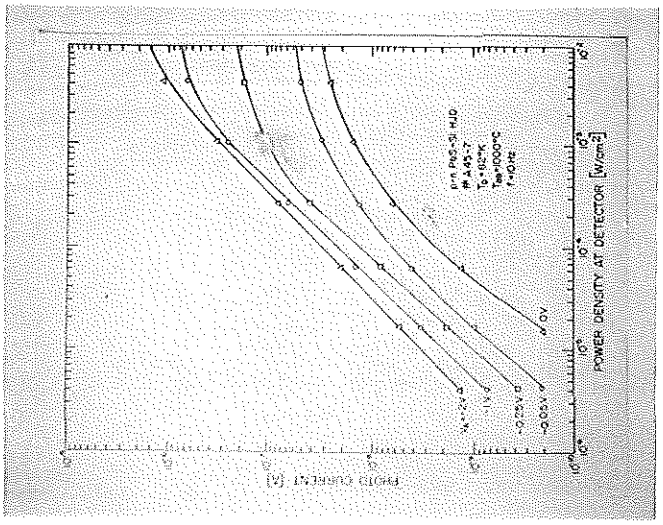

Fig. 6 Photocurrent vs. Power Density at f = 10 Hz

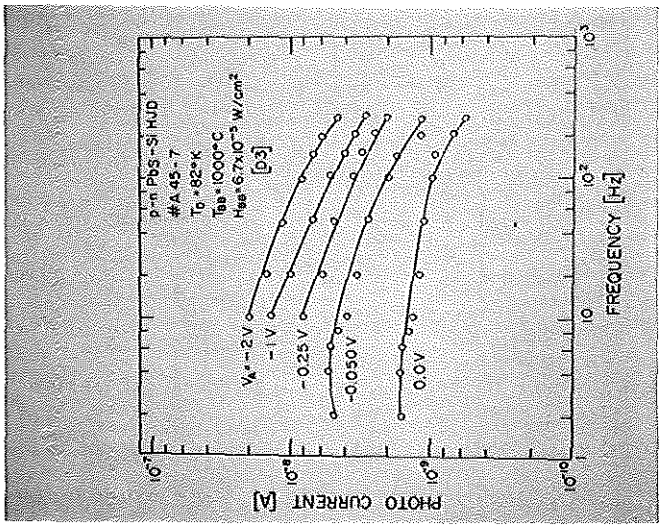

Fig. 7 Photocurrent Frequency Response at $6.7 \times 10^{-5} W/cm^2$

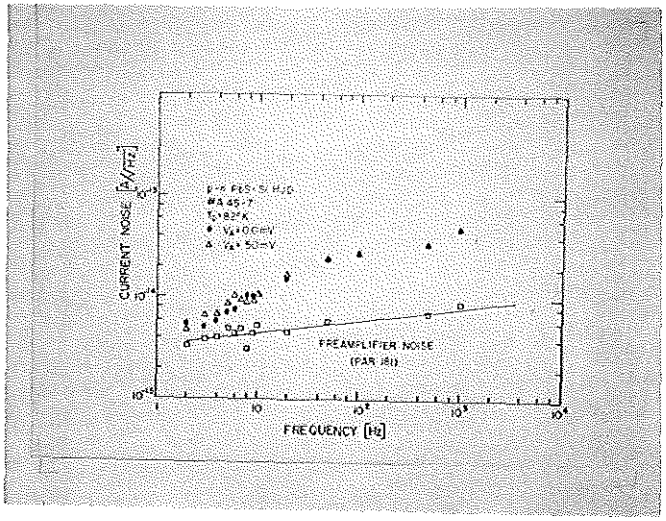

Fig. 8 Detector Current Noise

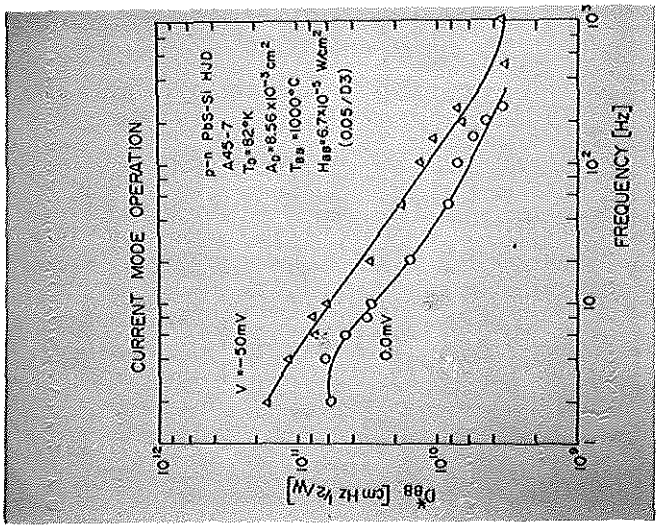

Fig. 9 Blackbody Detectivity for V_A = 0, -50 mV

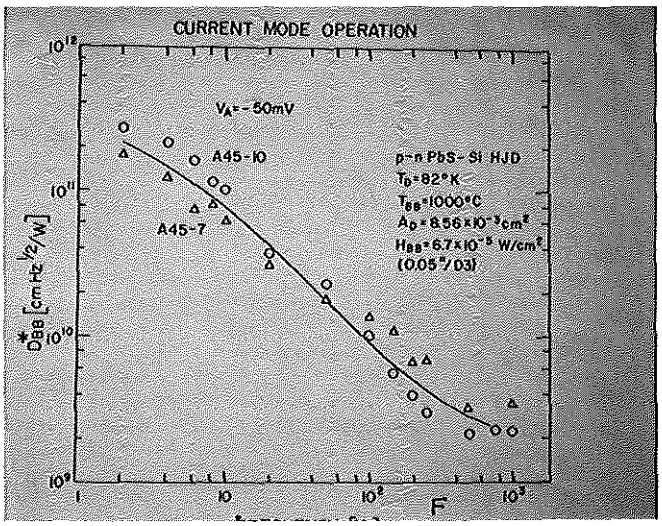

Fig. 10 Blackbody Detectivity for Two Detectors

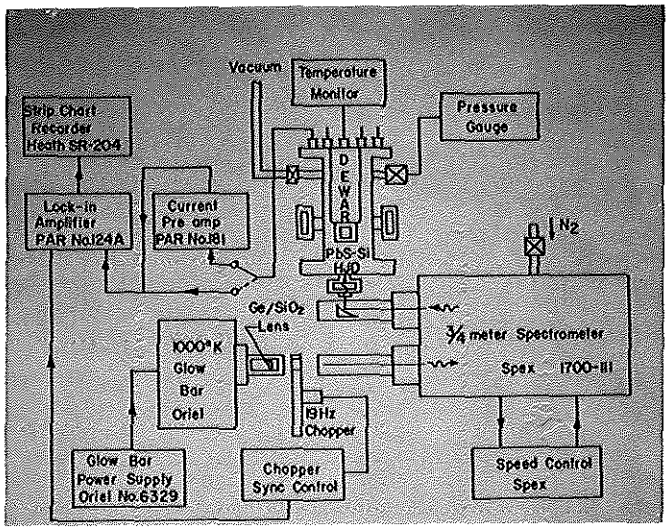

Fig. 11 Sprctral Response Test Station

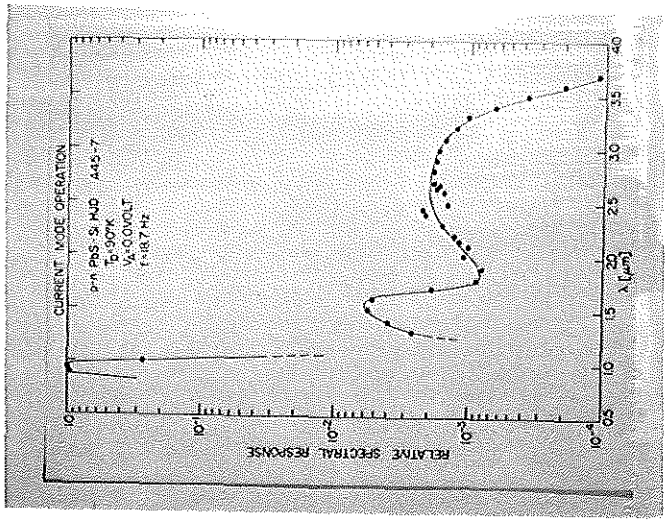

Fig. 12 Current Mode Spectral Response

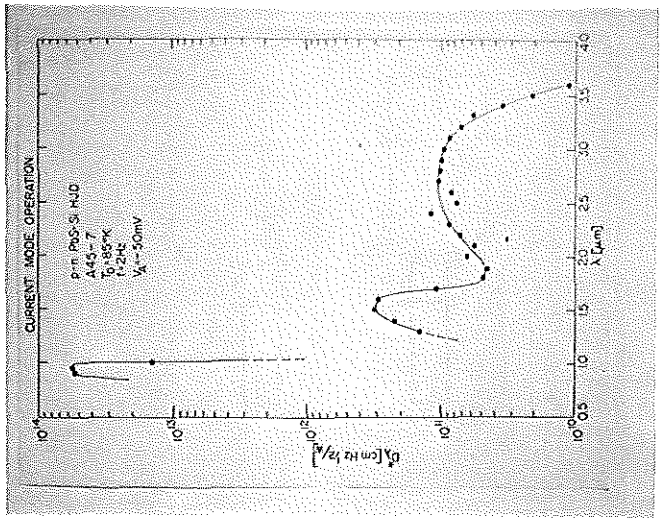

Fig. 13 Current Mode Spectral Detectivity

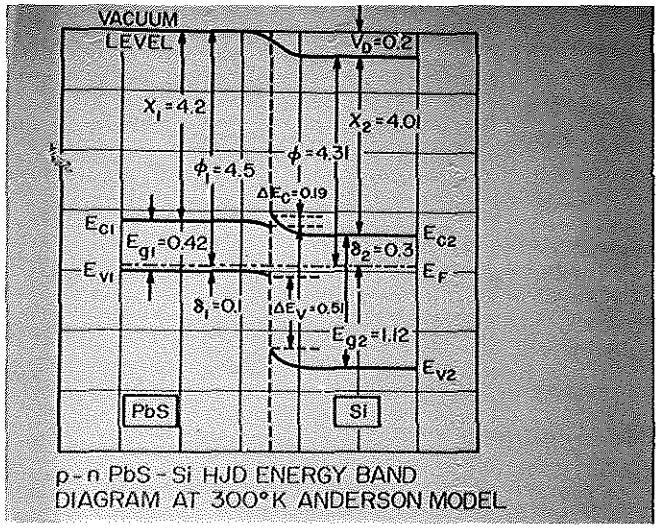

Fig. 14 PbS-Si HJ Energy Band Diagram

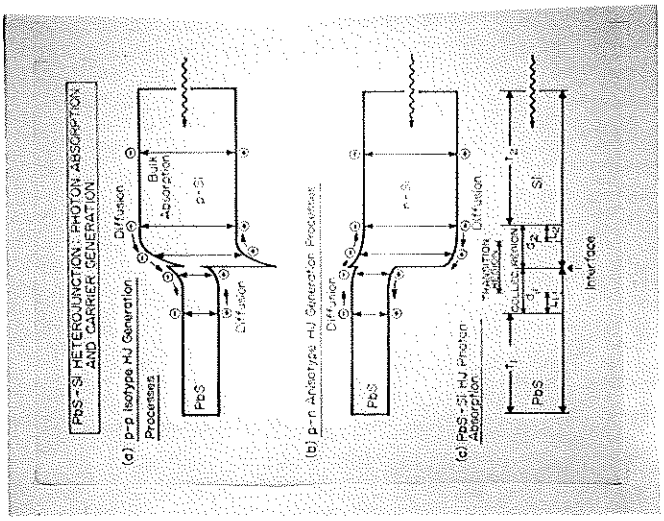

Fig. 15 Anisotype HJ Generation Processes

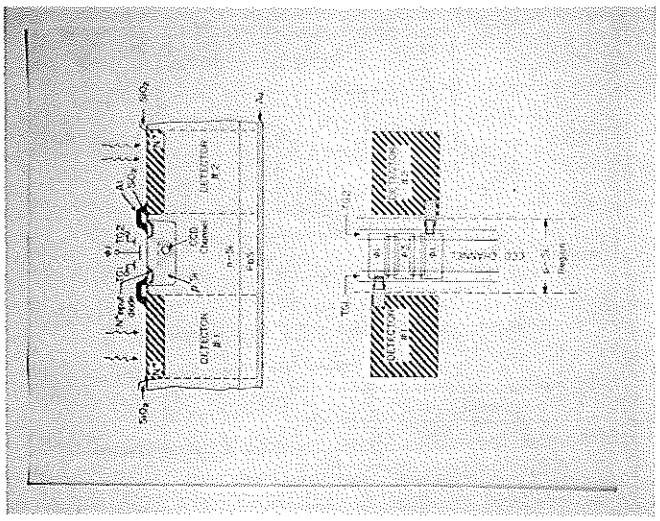

Fig. 16 PbS-Si CCD Integration

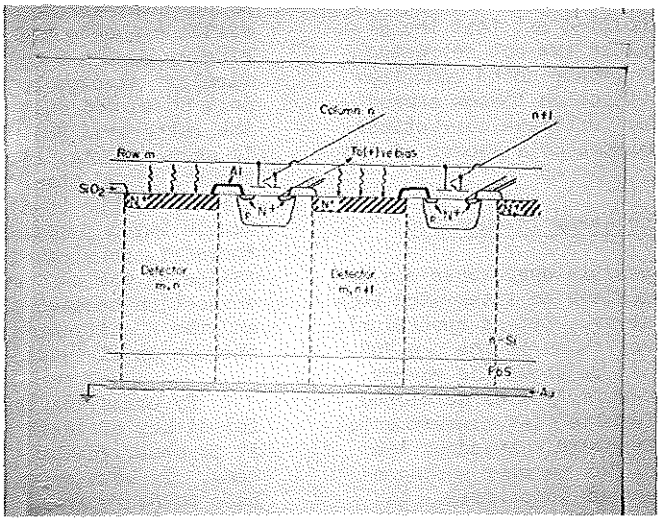

Fig. 17 PbS-Si MOS X-Y Integration

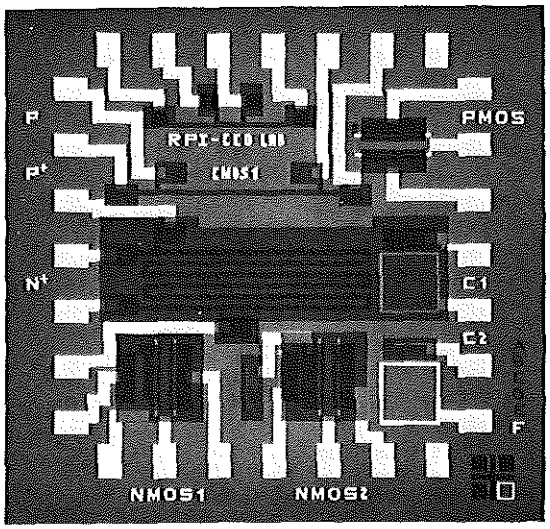

Fig. 18 CMOS Integration Chip

ly 2/3. Therefore by multiplying the curves of figures 9 and 10 by 2/3, the frequency response of D^*_λ (2.75 μm) can be observed.

It should be pointed out that the above detectivity values are not corrected for the substantial preamp noise contribution nor for the reflection losses caused by the dewar window. If these corrections are included an increase of a factor of two in D^*_λ is obtained.

IV. HJ Focal Plane Array Integration

A number of possible approaches can be taken in order to achieve an integrated PbS-Si HJ focal plane array. Let us specifically consider the integration of the p-n PbS-Si HJ. In Fig. 14 it is shown the energy band diagram of the anisotype HJ developed from experimental results (C-V measurements) and data in the literature. Based on the energy band diagram, the carrier photogeneration processes can be identified. As can be seen from Fig. 15, photoelectrons generated at or close to the interface result in the current which represents the infrared sensitive process. In reverse bias operation the Si substrate is held at a positive potential with respect of the PbS film, resulting in a dramatic photocurrent increase.

On this basis we have devised the integrated PbS-Si HJ CCD shown in Fig. 16. In Fig. 16a, the cross-section of the device is shown. Each HJ detector is connected through an Al interconnect to an input diode of the CCD register. The CCD is a n-channel device fabricated on a deep p-diffusion in the substrate. The HJ detector is effectively connected to the CCD channel through gate TG which also sets the bias on the detector. Since the CCD is n-channel, the polarity of the gate voltages will be positive, which is also the polarity required for reverse bias operation of the p-n PbS-Si HJ. In this fashion we will be injecting IR photogenerated electrons into the CCD and collecting them in the potential well under $\phi 1$. While only a very simple CCD input was used in this illustration, more versatile and more complex input circuits could be designed in order to implement such functions as background subtraction. A top view of the PbS-Si IRCCD is shown in Fig. 16b. In the particular design shown, two detector columns are accessed alternately by one CCD register in order to minimize dead space.

A second integration technique uses an array of MOSFET switches addressed by X and Y scan generators to read out the PbS-Si HJ detector array. A double-gated MOSFET switch connects each detector element to a single, common output. To read out a particular detector both gates of the switch must be turned on. The cross-section of the integrated PbS-Si HJ/MOS X-Y read-out is shown in Fig. 17. The cross-section of the PbS-Si HJ itself is that of the standard anisotype (p-n) PbS-Si structure. The double gated MOSFET switch is n-channel and therefore fabricated in a deep p-type diffusion on the n-Si substrate. The interconnection between the detector N^+ contact and the N^+ diffusion of the MOSFET is made through an Al interconnect.

By comparing the structure required for either of these integration approaches, it is observed that it is essentially the same. In both cases, n-channel circuits have to be implemented on an n-type substrate, thus requiring a p-well. We have therefore designed and fabricated a CMOS chip which contains the common basic structure and circuit required for the read-out of the integrated PbS-Si focal plane array. A photograph of the chip is shown in Fig. 18. The chip contains two devices designed to test the integration by either hard-wiring the detector output to the MOSFET input (NMOS1) or by a completely integrated structure (NMOS2). Also present on the chip are a p-channel device and test capacitors and resistors.

V. Conclusions

In this paper we have discussed the basic properties and the detector characteristics of the PbS-Si HJ. Detectivities of greater than 10^{11} cm $\sqrt{\text{Hz}}$/W have been reproducibly achieved. PbS-Si MOS integration structures have been discussed and a CMOS integration chip described. In conclusion, we feel that the PbS-Si heterojunction detector represents an attractive approach for the achievement of focal plane array integration in the 3μm region.

References

1. A.J. Steckl et al., "Application of Charge-Coupled Devices to Infrared Detection and Imaging", Proc. IEEE, 63, pp. 67-74, Jan. 1975.

2. J.L. Davis and M.K. Norr, "Ge-epitaxial PbS Heterojunctions", J. Appl. Phys., 37, p. 1670, March 1960.

3. H. Sigmund and K. Berchtold, "Electrical and Photovoltaic Properties of PbS-Si Heterodiodes", Phys. Stat. Sol., 20, pp. 255-259, 1967.

4. H. Elabd and A.J. Steckl, "Growth of PbS Polycrystalline Films", J. Vac. Sci. Tech., 15, p. 264, March 1978.

5. H. Elabd and A.J. Steckl, to be published.

6. A.J. Steckl, "Infrared Detector Properties of the p-p PbS-Si Heterojunction", Proc. IRIS Detector Meeting, 127200-3-X, pp. 277-287, March 1977 (Colorado Springs, CO).

7. A.J. Steckl, H. Elabd and T. Jakobus, "p-n Anisotype PbS-Si Heterojunction Characteristics", Tech. Digest IEDM, IEEE Cat. No. 77CH12757ED, pp. 549-550, Dec. 1977.

8. A.J. Steckl, M.E. Motamedi and S.P. Sheu, "Current Mode Operation of the p-n PbS-Si Heterojunction Detector", Proc. IRIS Detector Meeting, June 1978 (Annapolis, MD).